ELSEVIER

Biochimica et Biophysica Acta 1278 (1996) 147–159

BBA Biochimica et Biophysica Acta

Gramicidin channel-induced lipid membrane deformation energy: influence of chain length and boundary conditions

Avi Ring *

Department of Physiology and Medical Biophysics, Biomedical Centre, Box 572, S-751-23 Uppsala, Sweden

Received 4 July 1995; accepted 11 September 1995

Abstract

The influence of boundary conditions on the deformation energy of a lipid membrane containing a gramicidin A channel was evaluated numerically. A liquid crystal model was used to calculate the relative contributions of compression, splay and surface tension. It is proposed that the nearest neighbor lipid molecules are displaced from the channel end in a direction perpendicular to the bilayer and it is concluded that surface tension is the major component of the deformation free energy for monoolein (gmo)/n-alkane membranes. This unexpected result supports the validity of the liquid crystal models of membrane deformation since gramicidin lifetime has been shown to correlate with surface tension for gmo membranes. The theory accurately predicts the experimentally measured relative lifetimes without the use of adjustable parameters. For conditions where splay may be neglected surface tension is always the major component of the deformation energy, irrespective of the magnitude of the compression coefficient. The deformation may extend for hundreds of Å from the peptide. The results obtained here are expected to be important for the characterization of protein–membrane interactions in general.

Keywords: Lipid membrane; Gramicidin; Deformation free energy; Liquid crystal; Channel lifetime

1. Introduction

The mechanical properties of membranes have been described [1–4] and mathematical modelling of the interactions between membrane and protein has been attempted [2,4–14]. The hydrophobic mismatch [10] of a protein in a membrane and the lipid spontaneous curvature [8,14] have been suggested to be important determinants of the deformation free energy. There remains a considerable uncertainty in the physical and mathematical characterization of membrane–protein interactions.

The deformation properties of solvent-free lipid bilayer membranes have been modeled on the liquid crystal theory for a smectic with elongated molecules perpendicular to the plane [3,5,6]. The theory was applied to calculate the influence of membrane deformation on the gramicidin A channel lifetime [5,6,13]. It was concluded that compression of the lipid tails contributes significantly to the deformation free energy [5,6,15]. In a solvent-free membrane, compression was found to be the most important factor contributing to the deformation free energy [5], whereas surface tension energy was negligible.

For solvent-containing membranes the situation is more complicated. A lipid 'sandwich' with solvent in the middle has been used as a model for a solvent-containing membrane [16]. The deformation region close to the channel produces hard compression due to overlap of the lipid chains, whereas the region more distant to the channel produces softer compression [6].

For these solvent-containing membranes surface tension was found to contribute more to the deformation energy than the splay component but still significantly less than the compression component [6]. Thus, both Huang [5], and Helfrich and Jakobsson [6] found surface tension to be of lesser significance than the compression deformation energy. This conclusion is not compatible with the surface tension models of membrane deformation [17–22].

The liquid crystal models have not been able to explain the correlation of lifetime of the gramicidin channel with surface tension [17–22]. The earlier surface tension models, on the other hand, were empirical and could not explain the experimental results for the whole range of membrane lipids which have been used.

* Corresponding author. Fax: +46 18 174938; e-mail: aring@bmc.uu.se.

SSDI 0005-2736(95)00220-0

Two surface tension models [19,21] quantified the effect of the 'pull' of the membrane on the opening and closing processes of gramicidin channels. The model of Elliott et al. [21] has been referred to as the ENDH model. The model of Hendry et al. [19] is hereafter called the HUH model. In the HUH model, the free energy of deformation determines, through the Boltzman distribution, the ratio between open and 'closed' channels. In the ENDH model the deformation free energy increases the dissociation rate of the channel. The average lifetime is the inverse of the dissociation rate. In the ENDH model the lifetime is directly related to the component of the deformation free energy which depends on surface tension.

In both the HUH and ENDH models, surface tension is assumed to be the source of the channel destabilizing factor. The assumptions of the HUH and ENDH models were not compatible with the liquid crystal models since the latter models found surface tension to be of much lesser importance than the compressional energy. As is shown here, however, the large effects of splay and compression observed for the liquid crystal models critically depend on the membrane parameters that were assumed. Also, it is shown that the contribution of compression is sensitive to the choice of boundary conditions.

In the present report the theories of curvature elasticity of bilayers [3] and the hydrophobic mismatch theory [10] are combined to derive the differential equations. The only difference to the equations derived previously [5,6] is in the inclusion of terms involving the saddle splay and spontaneous curvature. These latter contributions, however, are not expected to be important for gramicidin in gmo/alkane membranes.

It will be shown that the empirical correlation of lifetime with surface tension is compatible with the liquid crystal model. This finding is important since it resolves the paradoxical inability of the liquid crystal models to explain the correlation of gramicidin lifetime with membrane surface tension. The results therefore support the usage of liquid crystal theory to model protein membrane interactions.

It will be shown that the theory predicts the relative lifetimes for gramicidin in gmo/hydrocarbon membranes. The fit to experimental data, without any adjustable parameters, is excellent.

Since the assumptions used for the boundary conditions are important for all membrane–protein interactions, it is of interest to investigate the influence of the choice of boundary conditions and lipid chain length on the relative contributions of compression, splay and surface tension in the case of the gramicidin channel. 'Relaxed' (see below) boundary conditions [13] are used in the numerical evaluation of the deformation free energy. It is found that the hard compression of the lipid tails adjacent to the channel may be relieved due to the slope of the membrane (Fig. 1, right).

The special case in which the splay contribution may be neglected is solved analytically for a membrane with a single stiffness-constant.

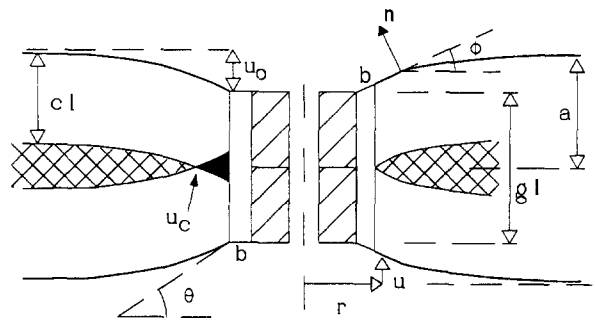

Fig. 1. Definition of **n**, R, r, r_1, u, u_c, u_o, b, ϕ, θ and boundary conditions for a gramicidin A channel in a lipid membrane with solvent (see also Table 1). On the left side of the channel the previously used boundary conditions are shown. The nearest neighbor lipid molecules are positioned at the same level as the channel end. R is the outer radius of the channel, cl is the chain length, b the nearest neighbor distance, a half the membrane hydrophobic thickness and gl the channel hydrophobic length. The hatched region is the solvent in the membrane interior and u_c is the deformation where the 'hard' compression of the lipid chains starts (black region illustrates overlapping chains). On the right side of the channel the boundary conditions proposed here are illustrated. The membrane slope is continuous up to the rim of the channel end. $r_1 = R + b\cos\theta$ is the beginning of the deformation region.

The results presented here differ from those of previous studies [5,6] and also from those of the HUH and ENDH models [19,21,22], but support the conclusion that the surface tension is the major component of deformation energy for the systems discussed and, unexpectedly, support the validity of the liquid crystal models [5,6].

2. Theory and numerical methods

A theoretical description of the deformation of a bilayer membrane containing a gramicidin A dimer channel has been formulated [5]. The deformation is assumed to be of circular symmetry. The differential equation relating the membrane deformation, u, in a direction parallel to the axis of the channel to the distance from the channel axis, r, was derived [5,6].

The theory was developed by analogy to a theory which was used to model the dynamics of liquid crystals. In the latter case an approximation of small perturbations was used [1] and the differential equations rest on the assumption that lipid molecules are locally perpendicular to the surface, i.e., tilt is not allowed. Also, it was assumed that the surface terms either may be neglected or integrate to zero over a closed surface. In particular, the total saddle splay (also called gaussian splay [25]) deformation energy is zero and therefore 'drops out' of the differential equations. The spontaneous curvature [3,8,14,24] was also not included in the theoretical description.

A membrane, however, has a large surface to volume ratio and it is not clear that the theory used for bulk liquid

crystals is valid in this case. Also, in the present case the monolayers are deformed in opposite directions (since gramicidin A is a symmetrical dimer). The small perturbation assumption (i.e., long wavelength compared to lattice spacing) is therefore also not appropriate. Nevertheless, the same model equations as proposed by Huang [5] may be derived using the theory developed to model vesicle shapes [3,23]. The compression term and the surface tension are included as proposed previously [5].

A bilayer and a vesicle differ with respect to two important issues. (1) The saddle splay deformation energy [3,24,25] integrates to zero over a closed shell whereas the total splay energy for a deformed bilayer is generally not zero. (2) It has been argued that the surface tension for a small vesicle is zero if the osmotic difference across the vesicle is zero [26]. This is not the case for a supported bilayer in contact with bulk lipid. (The question of a vanishing surface tension for a vesicle is not settled, however [27].)

The local curvature deformation energy density for each monolayer is assumed to be a quadratic function of the curvature. In complete analogy with the assumptions for a bilayer [3] the curvature energy density of a monolayer [8] is assumed to be

$$E_c = k_1(c_1 + c_2 - c_0)^2 + k_2 c_1 c_2 \quad (1)$$

To be compatible with earlier nomenclature we put $k_1 = aK_{spl}$ where a is the half bilayer thickness and for consistency $k_2 = aK'_{spl}$. c_1 and c_2 are the local principal curvatures and c_0 is the spontaneous curvature. c_0 is nonzero if the zero of free energy is not at a uniform orientation of the molecules [24].

The first term of Eq. (1) has been used [28] to model the phase behavior of phospholipid monolayer-lined cavities. For a situation with $c_0 = 0$ and $c_1 + c_2 = 0$ the only contribution to deformation energy is from the second term of Eq. (1). For such a situation $c_1 c_2 < 0$ (a saddle). It will be assumed that the saddle splay deformation energy is positive which is equivalent to assuming that there is no spontaneous warp in the monolayer, and therefore $k_2 < 0$, i.e., $K'_{spl} < 0$.

Reorganizing Eq. (1) gives, summing over both monolayers,

$$E_c = aK_{spl}(c_1 + c_2)^2 + aK_{spl}c_0^2 - 2aK_{spl}(c_1 + c_2)c_0 + aK'_{spl}c_1 c_2 \quad (2)$$

The first term corresponds to the term derived with the earlier approximations [1,5]. The present model for the curvature deformation density therefore differs from the earlier [5] only in the last three terms. The last two terms may give a significant contribution for other membranes (see Section 4) but are not of main concern for the results presented here. The second term contributes the same constant amount per unit area to both the undeformed and the deformed bilayer and therefore does not contribute to the protein–membrane interaction energy.

The third and last terms are independent of the shape of the membrane and depend only the on boundary conditions (see Appendix A).

Thus, if boundary conditions are chosen then the membrane shape may be determined using the same equations as were used previously [5,6]. The only difference will be that the total bilayer deformation energy is now obtained by integrating also the last two terms of Eq. (2). These terms may be obtained in a closed form. It is assumed that the initial slope of the membrane is S (the slope of the membrane at the channel, $S = \tan\theta$) and the integral of the last two terms of Eq. (2) (the spontaneous curvature and saddle splay components) is then (see Appendix A)

$$-4\pi aK_{spl}c_0 r_1 S - \pi aK'_{spl}S/(1+S) \quad (3)$$

where $r_1 = R + b\cos\theta$.

In practice c_0 and K'_{spl} are not known and their contributions will be discussed separately. In principle, however, given c_0 and K'_{spl} the total deformation energy is obtained in a straightforward manner. The method is the same as that used by Helfrich and Jakobsson [6]; minimizing the total deformation energy (including Eq. (3)) as a function of S. The shape of the membrane is then determined by the value of S at the minimum of the total energy.

The nomenclature used in this report is similar to that used previously. u is defined such that $u = 0$ at $r = \infty$ (for u and r see Fig. 1).

To summarize [5,6] the local compression, splay and surface tension components of the free energy per unit area of the bilayer are (including only the first term of the splay component, Eq. (2)),

$$F_{comp} = B_{soft}u_c^2/a + B_{stiff}(u - u_c)^2/(a - u_c) \quad (\text{for } u > u_c) \quad (4a)$$

$$F_{comp} = B_{soft}u^2/a \quad (\text{for } u < u_c)\ (u_c = a - \text{cl}) \quad (4b)$$

$$F_{splay} = aK_{spl}(u'/r + u'')^2 \quad (5)$$

$$F_{surft} = \gamma(u')^2 \quad (6)$$

where B_{soft}, B_{stiff} are the bulk module for soft and stiff elastic compression, γ is the interfacial tension (i.e., half membrane tension) and a is the half membrane thickness. u_c is the deformation threshold for stiff compression. cl is the lipid chain length.

The total free energy of the deformation is

$$F = 2\pi\int_{r_1}^{\infty} r\,dr\,(F_{comp} + F_{splay} + F_{surft}) \quad (7)$$

For minimum free energy $\delta F = 0$ and the Euler equation for the system is [5,6]

$$K_{spl}(u'/r^3 - u''/r^2 + 2u'''/r + u'''') - \gamma/a(u'/r + u'') + (B_{soft}/a^2)u = 0 \quad (8)$$

Eq. (8) holds for the region where $u < u_c$. For $u > u_c$ the last term is replaced with $B_{stiff}(u - u_c)/(a \cdot cl)$). Once a solution for Eq. (8) is found, the free energy is obtained from Eq. (7) by integrating the contributions Eqs. (4)–(6) and evaluating Eq. (3). To solve Eq. (8), boundary conditions must be chosen.

2.1. Boundary conditions

The boundary conditions used previously [6,19,21] assume that the lipid molecules closest to the channel are constrained in their vertical motion so that the membrane at the channel may not be thicker than the hydrophobic length of the gramicidin channel (Fig. 1, left side). This assumption stems from experimental observations of channel lifetime variation. The thickness of the membrane is altered by varying the constituents of the membrane. As the membrane is thinned and approaches the length of the channel, the deformation of the membrane decreases. It is then observed that the dimerized channel becomes more stable. When the thickness of the membrane equals the channel length, the dimer channel is not stabilized by a further thinning of the membrane. It has been concluded that the lipid molecules close to the channel have the hydrophilic head groups at the same height as the channel end. Then, if the membrane thickness equals the channel length there will be no deformation.

For a membrane which is thicker than the gramicidin channel length, however, we proposed previously [13] that the lipid molecules closest to the channel will be displaced in a direction parallel to the axis (see Fig. 1, right). This assumption is theoretically and experimentally justified. If the angle of the slope of the membrane is θ, and b is the distance along the membrane to the first lipid molecule, then the vertical displacement of the lipid from the channel end is $b\sin\theta$.

It should be noted that the justification for the boundary conditions used previously was the empirical lack of influence on lifetime of thickness variation for membranes of a thickness equal to the channel length. However, since the previous and present boundary conditions coincide when the membrane is flat ($b\sin\theta = 0$), the experimental findings for the thin membranes do not discriminate between the boundary conditions. With both the earlier and the present boundary conditions there will be no deformation of a membrane of thickness equal to the channel length and therefore no difference in the influence on lifetime. For thicker membranes, however, the difference in boundary conditions has important consequences. The contribution of lipid tail compression of the nearest neighbor lipids is significantly reduced with the present boundary conditions.

Theoretically, it is not likely that the nearest neighbor lipid head groups are positioned at the same level as the gramicidin hydrophilic end. Rather, it is expected that the slope from the channel end to the boundary lipid head group be nearly equal to (i.e., continuous with) that between the 'first' and 'second' lipids.

The distance between the nearest neighbor lipid head groups and the hydrophilic end of the channel (b above) is determined by the balance of forces between the head groups, the hydrophobic repulsion of the hydrocarbon-water contact and the entropy effects related to the mean free volume of the lipid chains [29]. For both sets of boundary conditions the nearest neighbor lipid is displaced from the channel due to the thermal motion of the tail. The nearest neighbor distance is not known, but is likely to be of the same order as the lipid-lipid distance (for gmo, 6 Å). A conservative assumption for the present purposes is to put $b = 3$ Å. With a channel outer radius (R) of 7 Å the radial coordinate of the first lipid is then about 10 Å, which is the same as that assumed for the previously used boundary conditions.

It is assumed that the molecular perturbations are sufficiently small to allow for a macroscopic description of the membrane [1,3,5] and that the effects of thermal fluctuations of the membrane thickness [15] may be either averaged or ignored. The effects of curvature and slope of the membrane on surface tension are not taken into account and we assume these effects will not significantly influence the conclusions.

The present hypothesis therefore gives the following boundary conditions (which will be referred to as the 'relaxed' boundary conditions)

$$u(r_1) = u_o - b\sin\theta \qquad u(\infty) = 0$$

$$\left.\frac{\partial u}{\partial r}\right|_{r=r_1} = \tan\theta = S \qquad \left.\frac{\partial u}{\partial r}\right|_{r=\infty} = 0 \tag{9}$$

where $u_o = a - gl/2$ is the membrane deformation at the channel (i.e., calculated as if the membrane were a continuum extending up to the channel entrance rim).

The hydrophobic length of the channel is about 21.7 Å, whereas the total length of the channel is about 26 Å [30,31].

2.2. Splay coefficients and spontaneous curvature

The value of the splay coefficient used here, $K_{spl} = 10^{-6}$ dyn [3,32], is the same as that used previously [5,6]. A greater value has also been given [33] but it was argued that the lower value is more correct [5,32]. In the present case an even lower value (favoring the conclusions of this report) should be appropriate. The presence of the solvent, which is partially sandwiched between the lipid layers [16] and partially between the lipid chains [34], is expected to lower the splay deformation energy and minimize effects from bilayer couple bending [25,35]. Furthermore, on theoretical grounds it was concluded [35] that the bending monolayer stiffness, which is appropriate here, is about 6 times lower than the bilayer couple stiffness.

The saddle splay coefficient, K'_{spl}, is not known. Both types of curvature deformations, symmetric and saddle shaped, are associated with lipid chain shape changes at constant lipid chain volume. It has been argued that generally K_{spl} and K'_{spl} could be expected to be of a similar magnitude [25]. Nevertheless, in the present case K'_{spl} should be significantly lower than K_{spl}. Both types of membrane deformation involve a molecular shape change at constant lipid chain volume. For K_{spl}, (the symmetric component of monolayer bending, i.e., with the same curvature in the x and y directions), a compressional splay of the lipid chains implies either (1) stretching of the lipid chains, or else (2) an increase in the surface area per lipid molecule. Either of these effects increases the bending energy in the deformation region. Either there will be an increased interference with lipid chains from the opposite monolayer (i.e., an increased contribution from elastic compression) or else there will be an increased exposure of hydrocarbon to water. (Close to the channel the compression stiffness is of the 'hard' type, see Eq. (4).)

In contrast to these effects for a symmetric deformation, a saddle splay deformation allows a lipid shape change at constant volume without chain stretching and with no change in surface area per lipid molecule.

With the convention adopted here the spontaneous curvature, c_0, for monolayers with PE/PC lipids is negative [28]. For gmo c_0 is expected to be close to zero. The shapes of the constituent molecules have been proposed to determine the stability of planar membranes [28,36,34]. Theoretically, gmo is considered to be a non-conical lipid and should therefore give membranes of low spontaneous curvature. Experimentally, it is well known that monoolein gives stable planar bilayers also at temperatures well above the main lipid phase transition (increasing temperature generally favors transition from the lamellar to the hexagonal phase). This finding supports the assumption of a low spontaneous curvature [32,34] and in the present case c_0 is not expected to have much influence on the total deformation energy. Further experimental support for a low energy contribution at zero curvature is the stabilization of the gramicidin A channel lifetime as the lipid thickness approaches that of the channel length.

As noted above (Eq. (3)), however, if the saddle splay coefficient and spontaneous curvatures are determined, their influence on the deformation free energy are readily included in the calculations.

Neglecting K'_{spl} and c_0 may not be adequate for phosphatidylcholine (DPPC) membranes but the approximation will be retained also for this latter case in order to facilitate comparison of the results obtained here (Figs. 2 and 3) (where modified boundary conditions are used) with the results presented previously [5,6]. DPPC lipid membranes also give stable planar bilayers, whereas phosphatidylethanolamine (DPPE) additions destabilize the lamellar phase increasing the tendency to form the hexagonal phase [28].

2.3. Minimization of the deformation free energy

Relaxation methods can be used to solve Eq. (8) and to calculate the deformation energy obtained as a function of the initial slope, S, of the membrane [6]. A different method was used here: a combined 'shooting'-minimization technique was used to obtain the shape of the membrane as a function of S. The integration of Eq. (8) requires four boundary conditions. The membrane deformation calculated at the channel, u_o, and the distance to the nearest lipid chain, b, are assumed to be given. In addition, the value of S is required for the boundary conditions given by Eq. (9) to be well-defined. Thus, the minimum energies and the corresponding values of S were obtained by the following steps:

1. a value of S (u' at $r = r_1$) was chosen.
2. Initial estimates were made for u'' and u''' at $r = r_1$ and Eq. (8) was integrated up to a sufficiently large value of r ($r = r_2$).
3. The integral represents a nonlinear vector function, $\boldsymbol{y} = \mathrm{f}(\boldsymbol{x})$, in which $\boldsymbol{x} = (u'(r_1), u''(r_1))$ and $\boldsymbol{y} = (u(r_2), u'(r_2))$. $\boldsymbol{y}$ is the prediction of the final values of u and u' (at $r = r_2$) given the initial values of u'' and u''' (i.e., at $r = r_1$). A root-finding package was therefore used to find the value of $\boldsymbol{x}$ (i.e., u'' and u''' at r_1) which solves the function f, i.e., results in zero derivatives at 'infinite' r. (The package automates iteration of step 2).

The root obtained defines the shape of the membrane compatible with (1) the differential equation (Eq. (2)), (2) the given initial slope, S, and (3) the requirement that the deformation and its derivative become zero at $r = r_2$. The energy components are then obtained by integration of Eqs. (4)–(6). This procedure was repeated for a range of values of S and the minimum energy, as a function of S, was determined (as described previously [6]).

The stiffness coefficient is discontinuous at $u = u_c$ and therefore for higher accuracy the integrals were performed in two steps. The first step extended from the channel and up to an r_m such that $u(r_m) < u_c$, and the second step from r_m to r_2. In the interval $r_1 < r < r_m$, $B = B_{stiff}$ for $u > u_c$ and $B = B_{soft}$ for $u < u_c$. In the interval $r_m < r < r_2$, $B = B_{soft}$ for the whole interval. In other words, stiff compression is ignored for large r even if in the process of minimization $u > u_c$. This procedure improves the speed of convergence and avoids getting trapped in local minima. Since the boundary conditions demand that $u = 0$ at 'infinity', putting $B = B_{soft}$ for large r has no bearing on the results.

Calculations were performed on a 486 AT. A general package for numeric computation (MATLAB, Mathworks, Natick, USA) was used.

3. Results

Fig. 2 shows the total deformation energy for a pc/decane membrane. The upper curves (continuous and dashed)

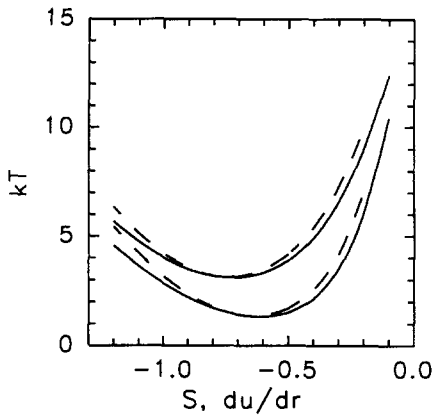

Fig. 2. Deformation free energy of a phosphatidylcholine membrane with a gramicidin A dimer channel as a function of the assumed initial slope of the membrane at the channel rim. The upper curves (dashed and continuous) are the solutions of the differential Eq. (8) with two different values of r_2, 120 Å and 300 Å, respectively. The upper curves were obtained with the same boundary conditions as those used by Helfrich and Jakobsson [6]. The lower pair of curves are for the boundary conditions given by Eq. (9).

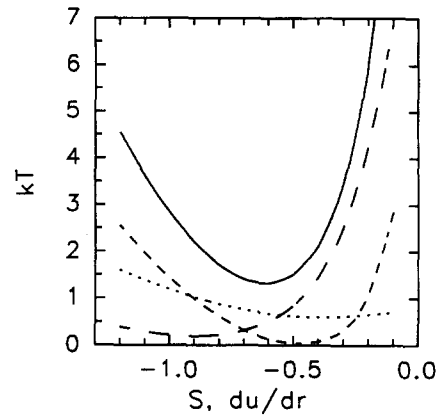

Fig. 3. Deformation free energy of a pc/decane membrane with a gramicidin A dimer channel incorporated, showing the contributions of surface tension (dotted), splay (short dash), compression (long dash) and total free energy (continuous). The parameters used are given in Table 1 (see text).

are the results for the boundary conditions used previously [6]. The upper curve therefore serves as a check for the present numerical techniques as well as a confirmation of the earlier results. The dashed and continuous curves represent results for r_2 = 120 Å and 300 Å respectively. The parameters used for the calculations are given in Tables 1 and 2.

The lower pair of curves shows the total energy ob-

Table 1
List of symbols

Symbol	Value	Units	Meaning
B_{stiff}	$5 \cdot 10^{-8}$	dyn/Å^2	stiffness (hard)
B_{soft}	$5.75 \cdot 10^{-11}$	dyn/Å^2	stiffness (soft)
K_{spl}	$1 \cdot 10^{-6}$	dyn	splay coefficient
K'_{spl}	–	dyn	saddle splay coefficient
b	3/0 [a]	Å	channel-lipid distance
R	7/10 [a]	Å	outer radius ($R + b = 10$)
a	half bilayer hydrophobic thickness		
c_0	intrinsic curvature of membrane		
c_1, c_2	principal curvatures of membrane		
cl	lipid chain length		
gl	channel hydrophobic length		
F	total deformation free energy		
$F_{comp/splay/surft}$	differential component deformation energies		
K_n ($n = -1,0,1,2$)	modified Bessel functions of the second kind		
n	unit vector perpendicular to membrane		
r	radial distance from axis of channel		
r_1	$r_1 = R + b\cos\theta$. Beginning of deformation region		
r_2	end point. r_2 taken as ∞		
r_m	termination point of first half of integral to obtain $u(r)$.		
S	initial slope of membrane = du/dr at r_1		
u, $u(r)$	membrane deformation at r		
u_c	a − cl (hard/soft compression boundary)		
u_o	a − gl/2 (membrane deformation at channel rim)		
z	monomer separation distance on channel breakup (ENDH)		
α	decay parameter for membrane deformation = $(a\gamma/B)^{0.5}$		
γ	half bilayer membrane tension		
ϕ	local angle of slope of membrane.		
θ	angle of initial slope = $\tan^{-1}(S)$		
τ	channel average lifetime		

The values for B, K_{spl}, gl and $(R + b)$ are the same as those used previously [5,6].
[a] Used for the calculation of 'non-relaxed' boundary conditions for comparison with earlier results.

tained when the new boundary conditions are used. It is clear that there is a significant lowering of the total free energy. For both sets of boundary conditions there is a negligible change in total energy at the minimum when the far boundary is increased from 120 to 300 Å. The change in S, however, is not negligible. Increasing r_2 allows S to become more positive, i.e., of decreasing magnitude. This change in S is intuitively clear, but the exact value of S at the minimum is not of concern here.

The details of the components of the continuous curve ($r_2 = 300$ Å) for the new boundary conditions are shown in Fig. 3. An unexpected result is that the surface tension (dotted) is the largest component of the total energy. This is in contrast to earlier conclusions [5,6] that surface tension was less significant in determining the shape and energetics of the deformation.

Fig. 4 compares the influence of the old (Fig. 4a) and the new (Fig. 4b) boundary conditions on the deformation energy for a thin, uncharged and virtually solvent-free membrane. The parameter values used here are the same as those used previously [6]; therefore the results can be directly compared. There is a significant lowering of deformation free energy when the relaxed boundary conditions are used. The lowering of deformation energy is, as for pc/decane in Fig. 2, of the order of 2 kT. In this case surface tension plays a minor role. The initial slope (S) at the minimum of free energy is of lower magnitude for the new boundary conditions and this is similar to the results for pc/decane.

The lifetime of gramicidin channels was measured for gmo/hexadecane [37] and gmo/decane [13] membranes. The gmo/alkane system has been used to model the influence of the physical properties of the membrane on the channel lifetime. It is therefore of interest to evaluate the deformation energy in these cases.

gmo/hexadecane membranes (Fig. 5a and b) are thin and relatively incompressible. Nevertheless, the surface tension is still the dominant component for the relaxed boundary conditions. In these membranes, the lowering of the energy is only of the order 0.5 kT when the nearest neighbor lipids are relaxed. The initial slope, however, is much lower than in the previous cases. Also, the deformation extends for hundreds of Å from the channel, and r_2 was therefore increased. The validity of the solutions were checked by comparing the results at the minimum for $r_2 = 300$, 350, 400 and 450 Å.

gmo/decane (Fig. 6a and b) is a thick compressible membrane in which decane occupies the interior of the membrane [16]. In this membrane the surface tension is the dominant component of the deformation energy for both sets of boundary conditions.

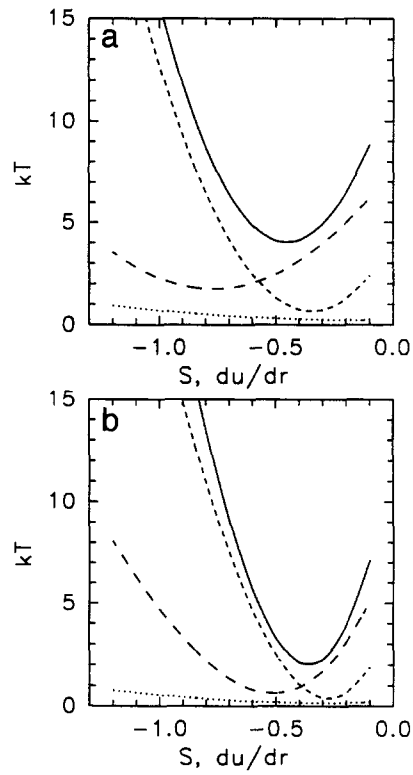

Fig. 4. Deformation free energy for a thin (28 Å) solvent-free membrane with a low surface tension coefficient $\gamma = 1.5$ mN/m. Curves are as for Fig. 3. Fig. 4a is for boundary conditions with $b = 0$ (see Eq. (9) and text) and Fig. 4b is for the same situation but with $b = 3$ (relaxed boundary conditions).

Table 2
Values of membrane parameters used in calculation of deformation energies

Membrane	a (Å)	γ (mN/m)	cl (Å)	r_2 (Å)
eic/squalene	14.25	$1.5 \cdot 10^{-8}$	14.25	120
gmo/hexadec.	15.5	$2.5 \cdot 10^{-8}$	12.5	300
gmo/tetradec.	19.35	$3.04 \cdot 10^{-8}$	12.5	350–400
gmo/dodec.	21.4	$3.45 \cdot 10^{-8}$	12.5	300–350
gmo/decane	22.5	$3.6 \cdot 10^{-8}$	12.5	350–450
gmo/octane	22.4	$4.38 \cdot 10^{-8}$	2.5	250
pc/decane	24	$0.8 \cdot 10^{-8}$	14.5	300

Values of a and γ for the gmo/squalene membranes are from [21]. Some membrane compression due to the electric field was assumed and the membrane compression was estimated from the data in [42]. 1.5 Å was used for gmo/decane and gmo/octane and smaller compressions for the thinner membranes. For eicosenoin/squalene without solvent no compression was assumed. a for gmo/decane is discussed in the text. eic is eicosenoin.

3.1. Comparison with experimental results for gmo/hydrocarbon systems

The deformation energy is only one of the components of the total activation energy for the breaking up process of the dimer. The deformation energy does not predict the magnitude of the lifetime. Nevertheless, the ratio of the lifetimes for two membranes may be predicted. If the solvent in the membrane is changed then, in general, the lifetime also changes. To model this change we assume

that the change in lifetime results from a change in deformation energy. Other membrane/channel interactions and the channel conformation are assumed not to change. The difference in deformation energies then predict the relative lifetimes. In Fig. 7 are compared the theoretically deformation energy differences with the corresponding values obtained from the experimentally determined lifetimes. The membrane is gmo with n-alkane solvents of solvent chain length $n = 8$, 10, 12, 14 and 16 carbons. The energy minima of Figs. 5 and 6 correspond to the predicted lifetimes for $n = 10$ and $n = 16$. The deformation energies for $n = 8$, 12 and 14 were calculated in an analogous manner. Values of the parameters are given in Table 2. In addition, the data of Fig. 4 correspond to those of eicosenoin/squalene which is a thin virtually solvent free membrane. The lifetime for eicosenoin/squalene was therefore taken as a reference; i.e., the lifetime was taken as unity and the energy minimum of Fig. 4 is used as the reference zero energy. The fit between the predicted energies and the experimental data (Fig. 7) is remarkable considering the fact that there are no adjustable parameters at all.

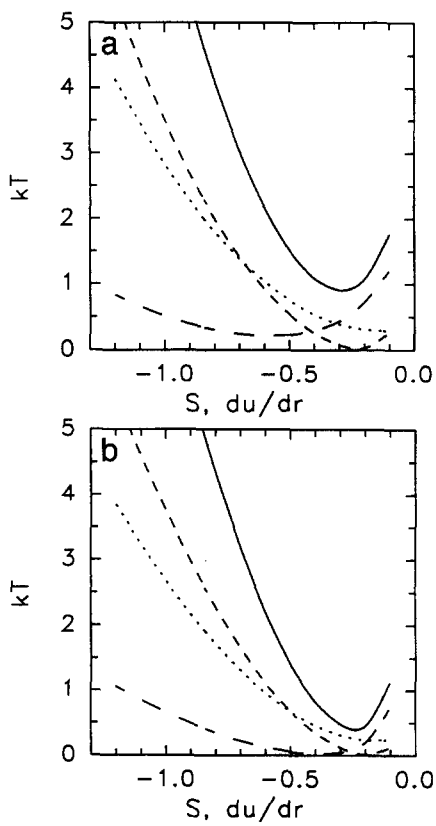

Fig. 5. Deformation free energy for gmo/hexadecane membrane. Fig. 5a is for $b = 0$ (see Fig. 4). Fig. 5b is for relaxed boundary conditions. Although the hexadecane membrane (32 Å) is thin (compared with gmo/decane, 45 Å), it does not give the same deformation energies as those of Fig. 4 (28 Å) also due to the significant differences in bilayer membrane tension for the two cases. Curves are as for Fig. 3.

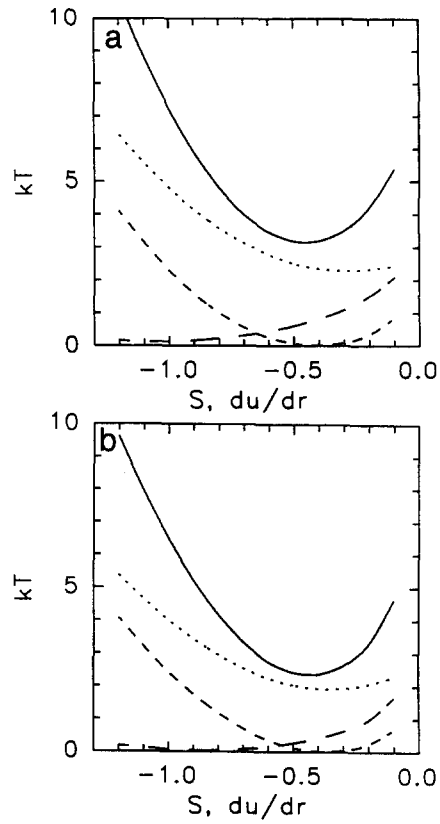

Fig. 6. Deformation free energy for gmo/decane membrane. (The thickness was taken as 45 Å since there is some compression due to electric field and increased salt strength.) Fig. 6a is for $b = 0$ (see Fig. 3), and Fig. 6b is for relaxed boundary conditions. Curves are as for Fig. 3.

3.2. For zero splay the surface tension always dominates the deformation energy

From Fig. 6b it is clear that the splay energy is negligible at the minimum of deformation free energy. The compression of the lipid chains at the channel is also small, partially due to the 'vertical' displacement of the nearest neighbor lipids. The membrane shape may then be obtained analytically. This solution was therefore also used as a check of the numerical integration method used above.

Thus, if the splay at the minimum is zero, K_{spl} may be set to zero and the solution is then given by (see Appendix B)

$$u(r) = AK_0(r/\alpha) \tag{10}$$

where K_0 is the modified Bessel function of the second kind, K_n, for $n = 0$ and $\alpha = (a\gamma/B)^{0.5}$.

For large x, $K_0(x) \approx e^{-x}/x$, and α, the coherence length, therefore determines the 'decay' of u and the range of the deformation. For the conditions in Fig. 6b: $B = 5.75 \cdot 10^{-11}$, $\gamma = 3.6 \cdot 10^{-8}$ and $a = 22.5$ (see Table 2). Then $\alpha = (a\gamma/B)^{0.5} \approx 120$ Å which explains the large extension of the deformations seen in the present case.

The incremental contributions to the deformation energy is proportional to $K_0(x)^2 + K_1(x)^2$ (see Appendix B)

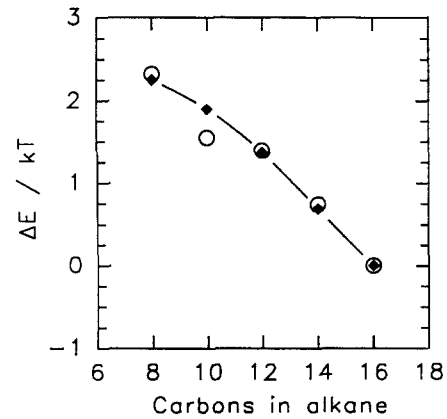

Fig. 7. Comparison of experimentally measured (○) and predicted (◆) lifetimes, τ, for gramicidin A channels in monoolein (gmo)/hydrocarbon membranes. No fitted parameters are used. The abscissae gives the number of carbon atoms in the alkane and the ordinate is the logarithm of (τ for gmo/n-alkane/τ for gmo/squalene) expressed as an energy in units of kT in accord with Eyring rate theory. The experimental values are from [21]. The theoretical values are obtained by the corresponding minima from calculation of the corresponding energy-shape curves (e.g., Figs. 4–6).

where the first term corresponds to compression and the second to surface tension. An immediate consequence is the surprising result that, since $K_1(x) > K_0(x)$, the surface tension component of the deformation energy is always greater than the compression component, irrespective of the relative magnitude of the compression modulus and the surface tension. This is in complete contrast to the conclusions from the earlier studies.

The total deformation energy is given by

$$F = \pi\left(\frac{B}{a}\right) r_1^2 A^2 \left(-K_0^2 - \left(\frac{\alpha K_1}{r_1}\right)^2 + \frac{(K_2 + K_0)^2}{4} \right) \tag{11}$$

where it is implicit that K_2, K_1, K_0 are functions of r_1/α. Although, paradoxically, the total deformation free energy is proportional to the compression coefficient, B, it depends on surface tension through the dependence of K_2 on α; as noted above the surface tension component is always the greater of the two. (It may be noted that the second term in Eq. (11), although proportional to γ through the factor α^2, does not explain the dependence of the deformation energy on γ, since this term is negative.)

As noted, the splay component of the deformation energy for gmo/decane with a gramicidin channel is negligible at the minimum (Fig. 6b). This means that Eq. (11) may also be used to evaluate the minimum deformation free energy for this system. The free energy was therefore reevaluated and the results verified the earlier numerical results for both the energy and the shape of the membrane.

The contribution of the splay deformation has been neglected in the surface tension models for all the lipid membranes used in previous studies [17–22]. Eq. (11) represents an approach which conforms to the same assumptions and was therefore used (below) to compare the predictions of the liquid crystal theory with those of the surface tension models.

4. Discussion

4.1. Surface tension may dominate the deformation energy

The excellent fit of the predictions of the theory to experimental data (Fig. 7) partially supports one of the major assumptions of the ENDH and HUH 'dimple' models [19,21,22]. It was postulated there that the surface tension energy in the formation of a dimer channel was the main factor involved in the differences in channel event activities observed in different membranes. It is interesting that the present finding of a large influence of surface tension at the same time also supports the liquid crystal model since the empirical correlation of lifetime with surface tension [17–22] were explained with the liquid crystal model.

The experimental results previously appeared not compatible with the predictions of the liquid crystal theory for solvent-free membranes. In the pioneering work of Huang [5], the deformation was calculated to be concave at the channel. Also, the deformation energy was dominated by compression and splay forces. The theory, for more general boundary conditions, was used [6] to show that the membrane shape could indeed correspond to that of a 'dimple' as suggested previously [17,19,21]. Although surface tension was now more significant, it was still not as important as the stiff elastic compression.

We conclude that these earlier results of the liquid crystal models are not valid for the solvent-containing membranes discussed here, since the surface tension component in all cases is here shown to be the most important factor in determining the deformation energy. For gmo/decane which is a thick, compressible membrane with a relatively large surface tension coefficient the surface tension component completely dominates the deformation energy.

The present results demonstrate the validity of the liquid crystal models. The results also show that the details of the boundary conditions and saddle splay, lipid-chain folding and effects of surface tension are important also for solvent-containing lipid membranes in general.

It should be noted, however, that the spontaneous curvature [3,8,14,24,36] may be of greater importance for membrane–protein interactions in the general case than what has been noted for the system under investigation here. For many biologically important lipid membranes such as PC/PE mixtures, the radius of spontaneous curvature may be as low as 30 Å. From Eq. (3) it may be estimated that the deformation energy is then several kT larger than with zero spontaneous curvature.

The spontaneous curvature may also explain the change in gramicidin lifetime observed in a series of experiments where the size of the polar head was decreased whereas the chain length and solvent were kept constant [18]. The lifetime decreased when the degree of methylation of the headgroup was decreased (from PC to PE). From the lifetime data given there it may be estimated that the decrease in lifetime would require an increase in deformation energy of about 1.6 kT. It is interesting that the increase in deformation energy is consistent with the measured increase in spontaneous curvature when PE is incorporated into PC membranes [28]. The magnitude of the resulting increase in deformation energy is predicted by Eq. (3).

From the same report [18] it may be concluded that increasing the lipid chain length also decreases the lifetime. The experimental data presented there show that when the chain length was increased then the lifetime decreased. The change in lifetime was larger, in general, than the changes observed when the head-group was changed. The data suggest that a change in lipid chain length may have more influence on the lifetime than the change in spontaneous curvature, a conclusion favoring the hydrophobic mismatch hypothesis [10].

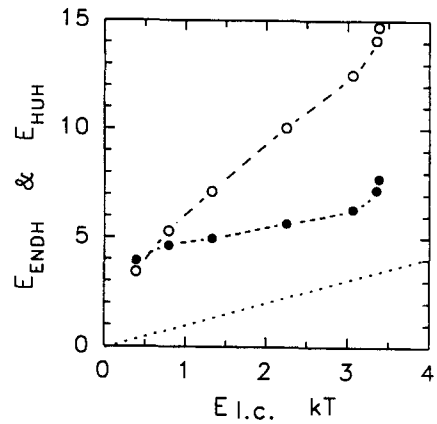

Fig. 8. Comparison of the deformation free energy of a membrane containing a gramicidin A dimer channel as calculated from Eq. (11), $E_{l.c}$, with the deformation energies in the approximate models used previously. Empty circles indicate the HUH model in which the deformation free energy is proportional to γu_0. Filled circles indicate the ENDH model in which the energy is proportional to $\gamma z \cos\theta$. Energies are in units of kT. The line of unit slope is for comparison with the liquid crystal model prediction. The curves are for visual aid only. The data used for thickness and surface tension are from Requena et al. [38]. The points ● and ○ are, in order of increasing energies, monoolein in hexadecane, tetradecane, dodecane, decane and heptane, respectively.

4.2. Comparison with the surface tension models

The equilibrium distribution of dimerized and non-dimerized gramicidin monomers is expected to depend on the deformation energy involved in the formation of channels. The conductance (G) of a bilayer is proportional to the number of open channels and G therefore depends on this equilibrium. G correlates with the surface tension over five orders of magnitude [19],

$$\log G = \mathrm{Log} G_0 - K\gamma u_0/kT \qquad (12)$$

where K is a parameter obtained by fitting to data.

In the ENDH model [21,22] the deformation energy is again proportional to the surface tension but now the lifetime, τ, of gramicidin is correlated with the deformation energy,

$$\log\tau = \log\tau_0 - K'\gamma z\cos\phi/kT \qquad (13)$$

where K' is a constant which depends on the radius of the 'well' created at the channel. z is the distance the monomers separate before breakup of the channel and ϕ is the angle the membrane makes with the channel axis. The values of z and ϕ were chosen to give the best fit to the data. (To obtain a good fit required a paradoxical value of 18 Å for z.)

Since the deformation energies have now been calculated analytically and are based on a general physical model of the membrane deformation, the values of the 'exact' result from Eq. (11) can be compared with the predictions from the more empirical ENDH and HUH models. In Fig. 8, Eq. (11) was used to calculate the deformation energies and these are compared with the ENDH and HUH models for a series of experimentally measured lifetimes. The bilayer tensions and thicknesses have been published by others [21,38].

The dotted line in Fig. 8 represents unit slope, i.e., calculated results should fall on this line for compatibility with the predictions of the liquid crystal model. The HUH model overestimates the deformation energy by more than 10 kT at the greatest deformation energies. The 'errors' in the predictions of the ENDH and HUH models are due to the assumption of a large curvature of the membrane at the channel which overestimates the surface tension contribution for thick membranes. In the liquid crystal model such a large curvature would be possible only if the compression coefficient is large. It is well known, however, that gmo/decane membranes are readily compressible, i.e., have a small compression coefficient [15,16].

In essence, however, the results from the present study support the central hypothesis of the surface tension models [17–22]. The present results show that surface tension is the major component of the deformation energy for solvent-containing monoolein membranes.

It is expected that for monoolein, as well as for shorter chains, the analytical result (Eq. (11)) should be a reasonable approximation of the deformation energy for a range of solvents. (In general, however, Eq. (11) must be used with care if it is not known whether the splay component can indeed be neglected.) It is therefore feasible to systematically compare the predictions of Eq. (11) with measured average channel lifetimes for these systems.

4.3. Deformation energy is sensitive to specific channel–membrane interactions

The liquid crystal model of Huang [5] is a macroscopic model in the sense that it presumes that the membrane is locally homogeneous [1,3]. It was shown here that the exact nature of the interactions of the nearest neighbor lipids and the channel, and therefore also the boundary conditions, determine the deformation energy of the membrane and thus the influence of the deformation on the kinetics of the protein.

Both dielectric and steric interactions are significant. From molecular dynamics simulations of the permeation properties of a gramicidin A channel, the dielectric interaction with the membrane of an ion occupying the channel was determined to be of the order of 10 kcal/mol [39]. We may therefore predict that the deformation region significantly influences the dielectric screening. The dielectric constant of the water which replaces lipid in the deformation region will result in a lowering of the deformation energy. Given that the total ion-membrane interaction energy is of the order of 20 kT, it may be that the calculated deformation energy may require significant correction. This situation for the open/close dynamics is similar to the discrepancies observed for molecular dynamics simulations of channel permeation. These simulations correctly predict the relative permeabilities of ions. Nevertheless, the permeation energy barrier profile was offset (too large) by an amount equal to the dielectric interaction energy.

This generalization, that the dielectric (and resonance) interaction energy observed on permeation will also influence the lifetime, is supported by the observation that the lifetime is influenced by the ion occupancy of the channel [37].

One simplification of the present theory is that dynamic interactions are not considered. For example, it has been shown that thermal fluctuations [40] change the effective rigidity of membranes with vanishing thickness and surface tension and in such systems the macroscopic rigidity may be lower than the microscopic rigidity. Including such effects is outside the scope of the present work but it is not clear that the assumptions are applicable in the present case. The results presented here are selfconsistent in the sense that the surface tension contribution is significantly larger than the splay contribution.

The possibility of a local tilt of the lipid molecules also can not be ignored. Generally, either the influence of tilt was not relevant or could be neglected in the applications of the theories of deformation of smectics [1,3,23]. For example, for vesicles a tilt of the lipid molecules is not possible [23]. In contrast, for the case discussed here, a planar bilayer with a local deformation, a tilt of the boundary lipids may be expected. The elastic energies of tilt are low [3]. Therefore, in general tilt may be important as a means for the boundary lipids to escape splay or compression deformation. This hypothesis is consistent with our conclusion of a relatively low contribution of the splay deformation energy in the present case.

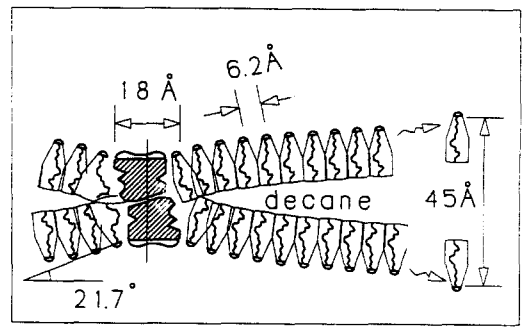

Fig. 9. Membrane deformation of gmo/decane membrane with gramicidin A dimer channel incorporated. The analytical solution to Eq. (10) and the numerical method were both used, independently, to calculate the shape. When the numerical method was used, splay, soft compression, stiff compression and surface tension were included in the calculation and S was set to -0.4 (Fig. 6b). The two methods of calculating the shape gave virtually identical solutions. The membrane deformation is long range. (The arrows on the right in the membrane indicate the asymptotic width of the membrane. The deformation extends for hundreds of Å as indicated by the broken arrows.) x and y scales are equal. The gramicidin hydrophobic length (shaded) is 22 Å and the monoolein chain length is taken as 12.5 Å (corresponding to half the width of a monoolein/squalene membrane). The lipids adjacent to the channel are likely to have shortened chains. This is shown on the left side of the channel. The hydrocarbon mean free volume is increased, however, corresponding to a loss of free energy, i.e., not to an increase of free energy due to compression. The space beneath the tryptophans also contributes to the increase in mean free volume of the nearest neighbor lipid tails.

Molecular dynamics simulations show that the lipid chains may avoid compression by folding under the tryptophans [41]. This means that Eq. (11) may be valid for a broader range of situations than is apparent when calculating the lipid chain compression from the thickness of the membrane, lipid chain length and length of the gramicidin channel. Generally it has been assumed that the compression of the lipids adjacent to the channel results from deformations in which the membrane becomes thinner than a solvent-free membrane with the same lipid constitution. If the nearest neighbor lipids may fold under the tryptophans, there will be no such compression.

The shape of the membrane deformation for gmo/decane with the gramicidin channel is shown in Fig. 9. The shape was constructed for $S = -0.4$ which is slightly lower than S at minimum energy in Fig. 6. The initial slope at the minimum in Fig. 6 is an upper bound on the actual value of the initial slope since mechanisms such as lipid chain folding (Fig. 9, left) will further decrease the effects of the hard compression. $u(r)$ for the construction of Fig. 9 was calculated using Eq. (8) and also using Eq. (11) but there was no significant difference in the shape (i.e., using a value of $S = -0.4$ and including splay and hard compression).

5. Conclusions

The theories of membrane deformation developed by Helfrich [3] and Huang [5] were combined to predict the deformation free energy of a lipid membrane with a gramicidin channel. The theory includes the effects of saddle splay and spontaneous curvature. Analytic expressions for these latter contributions were derived.

With the boundary conditions proposed here the lipid molecules may be displaced 'upwards' from the channel. This assumption results in a lowering of the hard compression component of the deformation energy. For gmo/*n*-alkane membranes the surface tension was shown to be the major component of the deformation free energy and the mathematical model was shown to predict the lifetime without adjustable parameters; this conclusion contrasts with previous conclusions. The remarkable fit and explanation of why earlier attempts have failed to demonstrate the empirical correlation of lifetime with surface tension supports the usefulness of the liquid crystal models.

An analytical expression for the deformation free energy was obtained for conditions of zero splay and a single stiffness constant; the theory then shows that surface tension is the major component of the deformation energy, irrespective of the membrane stiffness.

The deformation energy is sensitive to the details of the boundary conditions. The fact that the deformation region may extend over hundreds of Å for some systems is of significance to long-range protein–protein interactions.

The chain lengths, membrane thickness, surface tension and average channel lifetime for a number of lipid systems are known. If compressibility and splay coefficients can be estimated it is of interest to apply the theory to these systems. Comparing the results with experimentally obtained lifetime data will clarify the generality and limitations of the application of the liquid crystal model to bilayer membranes.

Appendix A. The contributions of spontaneous curvature and saddle splay to the total deformation energy

The last two terms in Eq. (2) may be rewritten expressing the principal curvatures in terms of the coordinates u, ϕ and r (see Fig. 1). (These coordinates were used previously in the calculation of vesicle shapes [3].)

Spontaneous curvature. If $\boldsymbol{n}$ is a unit vector perpendicular to the membrane (see Fig. 1) then the curvature in the directions x and y (local coordinates in the membrane along the principal directions of curvature) are $c_1 = \partial n_x/\partial x$, $c_2 = \partial n_y/\partial y$. The sum of curvatures is

$$c_1 + c_2 = \frac{\partial n_x}{\partial X} + \frac{\partial n_y}{\partial y} = -\left(\frac{\partial^2 u}{\partial x^2} + \frac{\partial^2 U}{\partial y^2}\right) = -\frac{1}{r}\frac{\partial}{\partial r}\left(r\frac{\partial u}{\partial r}\right) \quad (A.1)$$

and the deformation energy due to the spontaneous curvature (see Eq. (2)) becomes

$$-2K_{spl}c_0\int_{r_1}^{\infty} -\frac{1}{r}\frac{\partial}{\partial r}\left(r\frac{\partial u}{\partial r}\right)2\pi r\,dr = 4\pi K_{spl}c_0\left[r\frac{\partial u}{\partial r}\right]_{r_1}^{\infty} = -4K_{spl}c_0 r_1 S \quad (A.2)$$

Saddle splay. Expressing c_1 and c_2 using the coordinates r, ϕ

$$c_1 = -\cos\phi\frac{\partial\phi}{\partial r} \text{ and } c_2 = -\frac{\sin\phi}{r} \quad (A.3)$$

Then the saddle component of the deformation energy (last term of Eq. (2)) is

$$aK'_{spl}\int_{r_1}^{\infty} c_1c_2 2\pi r\,dr = aK'_{spl}\int_{r_1}^{\infty}\frac{\sin\phi}{r}\cos\phi\frac{d\phi}{dr}2\pi r\,dr = -\frac{1}{2}\pi aK'_{spl}[\cos(2\phi)]_{\theta}^{0} = -\pi aK'_{spl}\frac{S^2}{1+S^2} \quad (A.4)$$

where θ equals the initial value of ϕ (i.e., at $r = r_0$) and $S = \tan\theta$, the slope of the membrane at the channel.

Appendix B. The shape and energy of the deformation for a membrane when splay may be neglected

If $K_{spl} = 0$ then multiplying Eq. (8) by r^2 gives

$$r^2u'' + ru' - (B/a\gamma)r^2u = 0 \quad (B.1)$$

which is Bessels modified equation for $n = 0$.

The solution is conveniently expressed as

$$u = AK_0(r/\alpha) + A'I_0(r/\alpha)\ \left(\alpha = (a\gamma/B)^{1/2}\right) \quad (B.2)$$

where K_0, I_0 are modified Bessel functions of the second kind, K_n, I_n, for $n = 0$. The boundary condition $u \to 0$ as $r \to \infty$ demands that $A' = 0$ since I_0 diverges. A is not constrained by this boundary condition since $K_0(r) \to 0$ as $r \to \infty$. Instead, the solution is determined completely by the single boundary condition at $r = r_1$,

$$u(r_1) = (a - gl/2) - b\sin\theta = AK_o(r_1/\alpha) \quad (B.3)$$

where $\theta = |\tan^{-1}S|$. From Eq. (B.3) the initial slope, S, is

$$S = u'(r_1) = (1/\alpha)AK'_o(r_1/\alpha) = -(1/\alpha)AK_1(r_1/\alpha) \quad (B.4)$$

For the last equality use was made of

$$K'_n(x) = \frac{dK_n(x)}{dx} = -\frac{K_{n-1}(x) + K_{n+1}(x)}{2} \text{ and } K_{-1} = K_1 \quad (B.5)$$

Substituting $|\tan^{-1}S|$ for θ in Eq. (B.3) then gives a non-linear equation in A. (A is determined to within 0.5% in 2 iterations using Eqs. (B.3) and (B.4) and starting with $S = 0$.)

The deformation energies are obtained by integration of Eqs. (4) and (6) (and using Eq. (B.5) again)

$$F = 2\pi\int_{r_1}^{\infty} r\,dr\left((B/a)u^2 + \gamma u^2\right)$$

$$= 2\pi\gamma A^2\int_{\frac{r_1}{\alpha}}^{\infty} x\,dx\left(K_0^2(x) + K_1^2(x)\right) \qquad \text{(B.6)}$$

where $x = r/\alpha$ and the first and second terms correspond to compression and surface tension, respectively.

Eq. (B.6) may be integrated analytically. For any solution of Bessels modified equation, $x^2y'' + xy' - (x^2 + n^2)y = 0$, it can be shown that (differentiating each side)

$$\int_{x_1}^{\infty} xy^2\,dx = \frac{(x_1y')^2 - (x_1^2 + n^2)y^2}{2} \qquad \text{(B.7)}$$

Applying Eq. (B.7), with $x_1 = r_1/\alpha$, to both terms in Eq. (B.6) gives

$$F = \pi\gamma A^2\left(\left((x_1K_1)^2 - (x_1K_0)^2\right) + \left(\frac{x_1^2(K_2 + K_0)^2}{4} - (x_1^2 + 1)K_1^2\right)\right) \qquad \text{(B.8)}$$

where it is implicit that K_2, K_1, K_0 are functions of r_1/α and where the first and second terms in brackets correspond to the compression and surface tension terms, respectively. Collecting terms and resubstituting $r_1 = \alpha x_1$ gives Eq. (11)

$$F = \pi\left(\frac{B}{a}\right)r_1^2A^2\left(-K_0^2 - \left(\frac{\alpha K_1}{r_1}\right)^2\frac{(K_2 + K_0)^2}{4}\right) \qquad \text{(B.9)}$$

References

[1] De Gennes, P.G. (1974) The physics of liquid crystals, pp. 273–323, Clarendon Press, Oxford.
[2] Evans, E.A. and Skalak, R. (1979) CRC Critical Rev. Bioeng. 3, 180–419.
[3] Helfrich, W. (1973) Z. Naturforsch. 28C, 693–703.
[4] Sackmann, E. (1989) Can. J. Phys. 68, 999–1012
[5] Huang, H.W. (1986) Biophys. J. 50, 1061–1070.
[6] Helfrich, P. and Jakobsson, E. (1990) Biophys. J. 57, 1075–1084.
[7] Jähnig, F. (1981) Biophys. J. 36, 329–345.
[8] Kirk, G.L., Gruner S.M. and Stein, D.L. (1984) Biochemistry 23, 1093–1102.
[9] Marcelja, S. (1976) Biochim. Biophys. Acta 455, 1–7.
[10] Mouritsen, O.G. and Bloom, M. (1993) Annu. Rev. Biophys. Biomol. Struct. 22, 145–171.
[11] Owicki, J. and McConnel, H.M. (1979) Proc. Natl. Acad. Sci. USA 76, 4750–4754.
[12] Waugh, R.E., Song, J., Svetina, S. and Zeks, B. (1992) Biophys. J. 61, 974–982.
[13] Ring, A. (1992) Biophys. J. 61, 1306–1315.
[14] Keller, S.L., Bezrukov S.M., Gruner S.M., Tate M.W., Vodyanoy I. and Parsegian V.A. (1993) Biophys. J. 65, 23–7.
[15] Hladky, S.B., and Gruen D.W.R. (1982) Biophys. J. 38, 251–258.
[16] White, S.H (1980) Science 207, 1075–1077.
[17] Hladky S.B. and Haydon D.A. (1972) Biochim. Biophys. Acta 274, 294–312.
[18] Neher, E. and Eibl, H.J. (1977) Biochim. Biophys. Acta 464, 37–44.
[19] Hendry, B.M., Urban, B.W. and Haydon, D.A. (1978) Biochim. Biophys. Acta 513, 106–116.
[20] Rudnev, V.S., Ermishkin, L.N., Fonina, L.N. and Rovin Y.U. (1981) Biochim. Biophys. Acta 642, 196–202.
[21] Elliott, J.R., Needham, D., Dilger, J.P. and Haydon, D.A. (1983) Biochim. Biophys. Acta 735, 95–103.
[22] Elliott, J.R., Needham, D., Dilger, J.P., Brandt, O. and Haydon, D.A. (1985) Biochim. Biophys. Acta 814, 401–404.
[23] Deuling, H.J. and Helfrich, W. (1976) J. Physique 37, 1335–1345
[24] Frank, F.C. (1958) Discuss. Farady Soc. 25, 19.
[25] Fischer, T.M. (1993) Biophys. J. 65, 687–692.
[26] Tanford, C. (1979) Proc. Natl. Acad. Sci. USA 76, 3318–3319.
[27] White, S.H. (1980) Proc. Natl. Acad. Sci. USA 77, 4048–4050.
[28] Rand, R.P. and Fuller, N.L., Gruner, S.M. and Parsegian, V.A. (1990) 29, 76–87.
[29] Gruen, D.W.R. (1982) Chem. Phys. Lipids 30, 105–120.
[30] Urry, D.W., Goodall, M.C., Glickson, J.D. and Mayers, D.F. (1971) Proc. Natl. Acad. Sci. USA 68, 1907–1911.
[31] Koeppe II, R.E., Berg, J.M., Hodgson, K.O. and Stryer, L. (1979) Nature 279, 723–725.
[32] Engelhardt, H., Duwe, H.P. and Sackman, E. (1985) J. Physique Lett. 46, L395–L400.
[33] Schneider, M.B., Jenkins, J.T. and Webb, W.W. (1984) J. Physique 45, 1457–1472.
[34] Sjölund, M., Rilfors, L. and Lindblom, G. (1989) Biochemistry 28, 1323–1329.
[35] Fischer, T.M. (1992) Biophys. J. 63, 1328–1335.
[36] Israelachvilli, J.N., Marcelja, S. and Horn, R.G. (1980) Q. Rev. Biophys. 13, 121.
[37] Ring, A. and Sandblom, J. (1988) Biophys. J. 53, 541–548.
[38] Requena, J., Billet, D.F. and Haydon, D.A. (1975) Proc. R. Soc. Lond. A 347, 141–159.
[39] Åqvist, J. and Warshel, A. (1989) Biophys. J. 56, 171–182.
[40] Peliti, L. and Leibler, S. (1985) Phys. Rev. Lett. 54, 1690–1693.
[41] Xing, J. and Scott, H.L. (1989) Biochem. Biophys. Res. Commun. 165, 1–6.
[42] Andrews, D.M., Manev, E.D. and Haydon, D.A. (1970) Spec. Discuss. Farady Soc. 1, 46–56.